THE ASTROPHYSICAL JOURNAL, 316:611–625, 1987 May 15

THE FARADAY ROTATION OF CYGNUS A: MAGNETIC FIELDS IN CLUSTER GAS

J. W. DREHER AND C. L. CARILLI
Department of Physics, Massachusetts Institute of Technology

AND

R. A. PERLEY
National Radio Astronomy Observatory,[1] Socorro
Received 1986 September 24; accepted 1986 November 4

ABSTRACT

Multifrequency, multiconfiguration observations with the VLA have allowed, for the first time, detailed mapping of the rotation measure (RM) of the prominent extragalactic radio source Cygnus A. We find that this source lies behind a deep Faraday screen, with the rotation measure varying from −4000 to +3000 rad m^{-2} for the eastern lobe, and from −2000 to +1500 rad m^{-2} for the western lobe. Gradients in both lobes commonly exceed 300 rad m^{-2} arcsec^{-1}. The overall pattern in RM is the same in each lobe, increasing from east to west, leading to the conclusion that the magnetic field is ordered on scales of ~20 to 30 kpc. There is no evidence for internal depolarization. We examine, and reject, the hypothesis that this Faraday screen has a Galactic origin and propose that its origin is in the intracluster gas in which Cygnus A is embedded. Consideration of simple models gives cluster magnetic field strengths of from 2 to 10 μG. Although we have resolved the "rotation measure anomaly" of Cygnus A, we find we have a new mystery: what is the origin of the large-scale magnetic field in the intracluster gas?

Subject headings: galaxies: clustering — galaxies: intergalactic medium — magnetic fields — polarization

I. INTRODUCTION

Cygnus A is often considered the prototypical radio galaxy. It is the closest member of the class of high-luminosity, edge-brightened extended extragalactic radio sources. Its combination of high flux density, high brightness, and large angular size permits radio imaging of extraordinary detail in both total and polarized intensity. Cygnus A has been the subject of much observing by many authors (e.g., Mitton and Ryle 1969; Mitton 1971; Hargrave and Ryle 1974; Alexander, Brown, and Scott 1984), and the resulting images have figured prominently in our understanding of the origin and evolution of extragalactic radio sources. While these observations have demonstrated that Cygnus A displays a morphology typical for a high-luminosity radio source, they also showed that the polarization characteristics were highly unusual, even extraordinary. There seems to be no reason why Cygnus A should be unique with regard to its polarization properties, so these unusual characteristics in so prominent a radio source invite close attention.

Because of the prominence of Cygnus A to both observers and theoreticians, it seemed reasonable that a long-term, carefully executed series of observations using the Very Large Array (Thompson *et al.* 1980) would be justified. We have undertaken this program with the goal of producing the best images of this source, at all frequencies, resolutions, and polarization states allowed by the instrument. Early results in this program, based on the total intensity images at two frequencies, have been published by Perley, Dreher, and Cowan (1984, hereafter Paper I) and by Dreher, Perley, and Cowan (1985, hereafter Paper II). These showed the presence of a jet, leading from the nucleus into the western lobe, plus an unexpected, complex web of filamentary structure throughout both radio lobes.

In this paper, we give the results from a multifrequency analysis of the polarization data. Sections II and III give reviews of pertinent data from optical, X-ray, and radio-polarimetric observations. Section IV describes the new observations and discusses the problems in analyzing radio polarimetric data. The results are given in § V, and a discussion is in § VI. Section VII summarizes our conclusions. The Appendices contain details of the transfer of polarized radiation through ionized media, and models of the Faraday rotation in the Cygnus A cluster.

II. OPTICAL AND X-RAY OBSERVATIONS OF CYGNUS A

Optical observations have identified Cygnus A as an extremely large and luminous, narrow emission line cD galaxy, with $z = 0.0567$[2] (Baade and Minkowski 1954; Osterbrock and Miller 1975; van den Bergh 1976; Simkin 1977). The galaxy lies in a poor cluster, with velocity dispersion $\sigma_v = 2000$ km s^{-1} (based, however, on only five cluster members), leading to a central galaxy mass of $\sim 2 \times 10^{14}\ M_\odot$ (Spinrad and Stauffer 1982). Spinrad and Stauffer find the 26 mag red isophotes (uncorrected for reddening) extend out to radii of ~27″.[3] The absolute visual magnitude of the galaxy is unusually large: $M_v = -22.9$. Although Cygnus A lies at a Galactic latitude of only 5°.8, there is remarkably little Galactic absorption, estimated by Spinrad and Stauffer as $A_v = 1.09$ mag. Examination of the POSS prints reveals an almost total lack of nonstellar

[1] The National Radio Astronomy Observatory is operated by Associated Universities, Inc. under contract with the National Science Foundation.

[2] We use throughout $H_0 = 75$ km s^{-1} Mpc^{-1}, giving an angular scale of 1″ = 1 kpc.

[3] Using $A_r = 0.9$ mag, they derive a reddening-free 26 mag isophotal radius of 40″, although it is unclear to us, given their published photometry, how this was derived.

emission in the region, although, as expected, there is a very high density of stars. Attempts to detect optical emission corresponding to features in the radio lobes have proved fruitless (e.g., Kronberg, van den Bergh, and Button 1977).

Cygnus A is situated at the center of a very dense halo of X-ray emitting gas. Fabbiano *et al.* (1979) and Arnaud *et al.* (1984) show the X-ray emission comprises a centrally condensed region, of core radius ~ 130 kpc and central density ~ 0.01 cm^{-3}, and an extensive, diffuse halo extending out to 1.3 Mpc. The 2–6 keV luminosity is 2×10^{44} erg s^{-1}. Both the X-ray luminosity and the derived core gas density are among the highest known. Arnaud *et al.* have derived a density profile $\propto r^{-1}$ and have surmised the existence of a cooling flow of some 90 $M_\odot$ yr^{-1}. Similar cooling flows have been suggested for several other extremely luminous X-ray clusters. None of these clusters, however, contain a high-luminosity, classical double radio source.

III. PREVIOUS POLARIZATION OBSERVATIONS

Passage of linearly polarized electromagnetic radiation through a magnetized ionized medium results in a rotation of the plane of polarization at a rate

$$\frac{d\chi}{ds} = 0.81\lambda^2 n_e B_\parallel , \quad (1)$$

where χ is the position angle (PA), in radians, of the $\boldsymbol{E}$ vector of the radiation, n_e is the electron density in cm^{-3}, $B_\parallel$ is the component of the magnetic field parallel to the line of sight in μG, λ is the wavelength in meters, and s is the path length in parsecs. If the emitting region lies entirely behind the ionized medium, the solution to equation (1) is $\chi(\lambda) = \chi_0 + \mathrm{RM}\lambda^2$, where χ_0 is the value of χ incident on the ionized region, and RM, the rotation measure, is a constant given by $\mathrm{RM} = 0.81 \int n_e B_\parallel \, ds$. A distinctly different behavior occurs if the ionized medium lies within the emitting volume, as described in Appendix A. The position angle of the plane of polarization is an observable quantity, and considerable effort by many observers has gone into measuring the RM for hundreds of radio sources (e.g., the compilation of Simard-Normandin, Kronberg, and Button 1981 includes data from 53 references and gives the RM for 555 extragalactic radio sources).

The so-called "rotation measure anomaly" of Cygnus A was first identified by Mitton (1971). Using his own and others' observations (mainly with single antennas), of the integrated polarized intensity of each lobe at wavelengths ranging from 1.5 to 6.4 cm, Mitton found RM values for the western and eastern lobes of 35 rad m^{-2} and -1350 rad m^{-2}, respectively. The latter value was higher than any seen before in an extragalactic radio source and was rendered even more notable by the great difference over the small angular distance ($\sim 1\rlap{.}'5$) between the lobes. In addition, a considerable decrease in the degree of polarization, integrated over the lobes, with increasing wavelength was noted: from $\sim 10\%$ at 15 GHz to $\sim 2\%$ at 5 GHz.

Later polarimetric imaging of Cygnus A, using aperture synthesis techniques, produced more evidence that large and complicated Faraday effects were occurring. The 2″ resolution 5 GHz maps of Hargrave and Ryle (1974), showed the existence of areas of high percentage polarization (up to 25%) within the radio source. These data, roughly combined with 23 GHz data at 6″ × 10″ resolution by Dreher (1979), were consistent with RM values at the hot spots found by Mitton. More recent 2.7, 5, and 15 GHz maps of the source at 4″ resolution by Alexander, Brown, and Scott (1984) showed apparent large depolarization with increasing wavelength. They experienced difficulties in determining the RM distribution across the source but reported RM values in the eastern lobe which varied from -1100 rad m^{-2} at the hot spot to -250 rad m^{-2} in the lobe tail region. Their RM data for the western lobe appeared "noisy," with "no overall pattern" discernible.

The primary point of interest is the location of the gas giving rise to the observed large Faraday rotation. Three possible locations discussed by previous authors are (1) our Galaxy, (2) the Cygnus A cluster, and (3) internal to the radio source. A Galactic origin is supported by the low Galactic latitude of Cygnus A and was addressed in detail by Mitton (1971). He concluded that the Galaxy can be expected to contribute ~ 250 rad m^{-2} to the observed RM, far short of the required amount. He suggested that the remainder of the RM arose from a screen composed of U-shaped or helically shaped fields wrapped about, and partially within, the radio lobes. Recently, Alexander *et al.* have revived the possibility of a Galactic origin for the observed RM, citing the Galactic H I absorbtion across the source observed by Greison (1973) as an indicator of intervening Galactic material. Slysh (1966) considered an extragalactic location for the Faraday screen, proposing a massive "halo" of ionized gas enveloping the optically observed galaxy as a possible site for the gas. Dreher (1979) suggested that there might be a Faraday screen near Cygnus A and that gradients in the RM greater than ~ 300 rad m^{-2} arcsec^{-1} could explain some of the apparent depolarization between 23 and 5 GHz. The third location, internal to the source, was considered by Hargrave and Ryle (1974). They suggested that the apparent low percentage polarization at 5 GHz in some regions of their 2″ resolution maps could be due to Faraday depolarization by internal thermal gas, and they inferred an internal thermal gas density of $\sim 10^{-3}$ cm^{-3}. From the failure of their 2.7 GHz maps to conform to the RM suggested by Mitton (1971), De Young, Hogg, and Wilkes (1979) also suggested the presence of thermal gas inside the lobes.

IV. THE NEW OBSERVATIONS

From the discussion of the preceding section, it is evident that the origin of the anomalous polarization of Cygnus A remained quite unclear. With the completion of the VLA, an opportunity arose to measure the polarization at many frequencies, with unprecedented sensitivity and resolution. One of the goals of our study of this source has been, therefore, to settle the issue of the character of the polarization and the location of the magnetoactive region.

As is well known, determination of the rotation measure is complicated by $n\pi$ ambiguities in the observed PA. Removal of these ambiguities requires observations at many frequencies, two of which, at least, should be close enough in wavelength to eliminate the possibility of any ambiguity within a reasonable rotation measure range. With an RM of ~ 1000 rad m^{-2}, a rotation of ~ 1 radian is expected between 4500 and 5000 MHz, the approximate frequency range of the VLA 5 GHz band. Use of data taken at these frequencies allows an unambiguous determination of the rotation measure if $|\mathrm{RM}| \leq 1300$ rad m^{-2}, larger than the anticipated values. Data at 15 GHz provide a valuable check to the correctness of any RM determination made at lower frequencies, increase the precision of the RM measurements, and are necessary to determine the degree of depolarization at 5 GHz.

The VLA allows full polarization observations at two frequencies simultaneously, providing they lie within the same band (e.g., 5 GHz band, or 15 GHz band). We thus observed Cygnus A with all four configurations of the VLA at 4525 MHz and 4995 MHz, and with the "B," "C," and "D" configurations at 14945 and 14655 MHz, as summarized in Table 1. After initial imaging, we realized that the magnitude of the rotation measure, in certain areas, was considerably greater than 1300 rad m^{-2} and another frequency within the 5 GHz band was required to eliminate ambiguities. Fortunately, our earlier observations (Paper I) were taken at 4886 MHz, and inclusion of these data enabled rotation measures of up to 9650 rad m^{-2} to be determined unambiguously.

During the analysis of this data, it also became clear that a determination of the RM of the nearby calibrator source 2005+403 would be useful to assist in the interpretation of the results from Cygnus A. These observations were taken in 1985 August, in the "C" configuration, at four frequencies each in the 1.5 GHz and 5 GHz bands, and two frequencies in the 15 GHz band. The frequencies were chosen to eliminate any reasonable possibility of ambiguities in the determination of the rotation measure.

All of the data were calibrated using periodic observations of 2005+403. The flux density scale was based on the Baars *et al.* (1977) scale through observations of 3C 286. The antenna polarizations were calibrated using 2005+403, and the true position angles of the polarized flux density were set through observations of both 3C 286 and 3C 138, for which position angles of 33° and −12°, respectively, were assumed at 5 GHz, and 33° and −18° at 15 GHz. The techniques used for calibration were standard, and no unusual problems were encountered. After this calibration, all data of the same frequency but different configurations were combined. All 15 GHz data were combined, as the Faraday rotation between the two 15 GHz frequencies is negligible.[4] Following concatenation, the data were processed using the "AIPS"[5] software package. The usual procedures of editing and self-calibration were followed, then images at various resolutions in Stokes parameters I, Q, and U were made and deconvolved. The deconvolution algorithm used was "CLEAN" (Högbom 1974; Clark 1980), except for the highest resolution I image at the 5 GHz band, where the maximum entropy algorithm, "VM", was used (Cornwell and Evans 1985). In this case, the results were convolved with a 0".35 Gaussian to mimic the "CLEAN" beam used for the corresponding Q and U images.

For reference, we show in Figure 1 an image of Cygnus A at 5 GHz with 1" resolution, using the data taken for these observations. Note the central nucleus, separated lobes, and prominent hot spots—all features of a high-luminosity radio source. The jet and filaments are poorly represented here. See Paper I for details on these features.

From these "primary" images, maps of the polarized intensity, $P = (Q^2 + U^2)^{1/2}$, degree of polarization, $m = P/I$, and position angle of polarized intensity, $\chi = \frac{1}{2} \arctan (U/Q)$, were made. Finally, maps of the depolarization ratio, $D = m_2/m_6$, were made by dividing the 15 GHz degree of polarization map by the 5 GHz degree of polarization map.

There are two important sources of error to consider when interpreting depolarization maps. The first concerns the propagation of error. An elementary calculation, assuming only quadratic summation of noise, gives

$$\delta D = D[(\delta_{m_6}/m_6)^2 + (\delta_{m_2}/m_2)^2]^{1/2} , \qquad (2)$$

where m represents the degree of polarized flux density, $D = m_2/m_6$, δ is the rms noise in the subscripted quantity, and the numerical subscript refers to wavelength. Thus, to measure a depolarization to $\delta D/D = 0.05$, both input maps must have a signal greater than 30 times the noise, if each map contributes equally to the output error. For Cygnus A, the errors, δm, are usually small, but in areas in which m is also small the effective error is magnified. Fortunately, although such regions of low m are prevalent, there are many areas, especially in the western lobe, in which high signal-to-noise ratio can be obtained, and accurate determinations of the depolarization are possible. Note that, although the degree of polarization may be low over much of Cygnus A, the polarized intensity is still well above the noise, so that we can ignore the effects of the bias introduced by the positivity of the polarization intensity maps (e.g., Wardle and Kronberg 1974; Killeen, Bicknell, and Ekers 1986; Simmonds and Stewart 1985).

A second and very important source of error in determining the depolarization is that due to rotation of the plane of polarization across the synthesized beam. This results in an apparent reduction in the observed fractional polarization of the radiation. Such a rotation can occur in two ways: (1) The

[4] Trial RM images, utilizing only the 15 GHz data, were made to determine whether RMs > 10^4 rad m^{-2} were present. No evidence for such large RMs was found. The resulting maps confirmed the trends seen at 5 GHz, but were of lower precision.

[5] AIPS is an acronym for Astronomical Image Processing System, a software system developed by the NRAO for calibration, imaging, and analysis of astronomical data.

TABLE 1

OBSERVING LOG OF CYGNUS A OBSERVATIONS

Observing Date	Configuration	Observing Frequencies (MHz)	Bandwidth (MHz)
1980 Feb 24	Mixed	1446, 4886	12.5
1982 Jun 20	A	1446, 4886	6.25
1982 Oct 25	B	1446, 4886	12.5
1982 Oct 28	B/D	1446, 4886	12.5
1983 Feb 2	C	4885	50
1983 Oct 23	A	4995, 4525	6.25
1984 Jan 14	B	4995, 4525, 14655, 14945	12.5
1984 Jan 23	B	4995, 4525, 14655, 14945	12.5
1984 Apr 15	C	4995, 4525, 14655, 14945	12.5
1984 Apr 23	C	14655, 14945	12.5
1984 Apr 24	C	14655, 14945	12.5
1984 May 24	C	14655, 14945	12.5
1984 Aug 28	D	4995, 4525, 14655, 14945	25

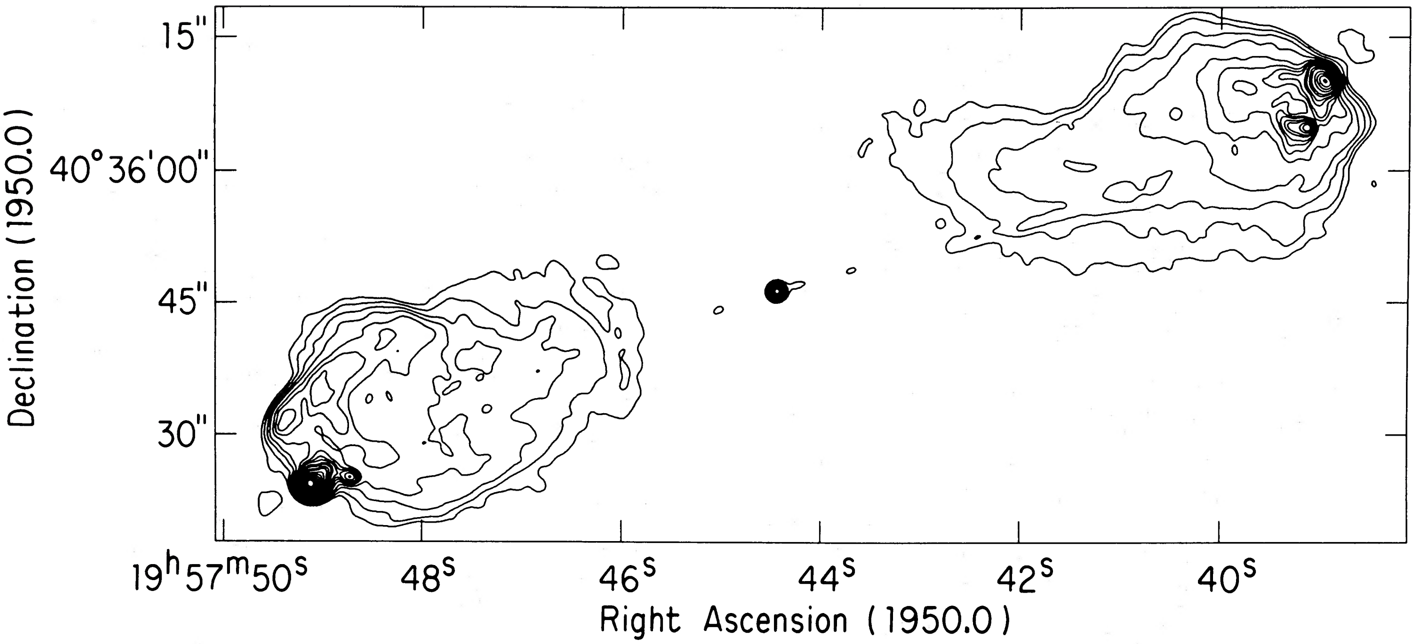

FIG. 1.—Cygnus A at 5 GHz with 1" resolution. The contour levels are at 0.075, 0.2, 0.5, 1, 2, 3, 4, 5, 7.5, 10, 15, 20, 30, . . . , 80, 90% of the maximum brightness of 14.5 Jy per beam. The morphological features displayed here are typical of high-luminosity radio sources. The jet and filaments are best seen in a gray-scale plot, especially at high resolution, such as in Fig. 4. See Fig. 1 of Paper I.

source geometry is such that the intrinsic emission changes on such scales, and (2) a Faraday screen causes differential rotation. That is, there exists a rotation measure gradient sufficient to cause beam depolarization. Of course, both effects can be operating at the same time, resulting in either a worsening, or improvement, of this depolarization. The first effect will not cause the fractional polarization to change with frequency, unless there also exists a substantial spectral index change across the beam. The second effect is much more pronounced at lower frequencies, and, hence, will cause a strong frequency-dependent depolarization. An accurate estimate of the internal depolarization thus requires the rotation measure to be suitably uniform across the synthesized beam. For a rough estimate of beam depolarization, we can approximate the beam as a top hat, across which the position angle of polarized flux density rotates by angle η. The apparent depolarization in this case is $\sin \eta/\eta$. From this, it follows that to keep the instrumental depolarization to less than 5%, $\eta < 28°$ is required, which at 5 GHz translates to a change in rotation measure of less than 135 rad m^{-2} over the angular scale of the beam. Few regions of the eastern lobe met both this requirement and that of the preceding paragraph. Many areas of the western lobe met both criteria however, so good measures of D were possible for this lobe.

Because the observed position angle is, to first order, unaffected by modest rotation of the plane of polarization across the synthesized beam, an accurate estimation of rotation measure can be made even in the presence of beam depolarization.

Images of rotation measure were constructed by solving for the best-fit slope of position angle χ versus λ^2. To do this, a special "AIPS" program was written to read a data cube whose top four planes consisted of the position angle maps and whose bottom four planes were the corresponding error maps. These errors were calculated assuming simple quadratic summation of noise from the Stokes Q and U images, $\sigma_U/2P$, assuming (as should be the case) that the errors in Q and U are equal. The program runs in the following way: For every pixel, an initial guess of the rotation measure is made, using only the data at 4995 and 4885 MHz. It is *assumed* that the two position angles lie within $\pi/2$ radians, i.e., there are no $n\pi$ ambiguities between the two. This assumption is valid if $|\mathrm{RM}| \leq 9650$ rad m^{-2} for this frequency pair. Next, this initial guess of the rotation measure is used to remove ambiguities from the 4525 MHz datum by adding or subtracting multiples of π until the difference between the predicted and measured value is less than $\pi/2$. A three-point weighted least-squares fit follows, from which ambiguities in the 15 GHz datum are removed. Finally, a four-frequency weighted fit is made. This fit determines both the rotation measure and the intrinsic polarization angle of the electric field. From the latter, the projected magnetic field is derived by adding 90°. In practice, fits for any pixel were attempted only when all four input data points had associated errors less than 10°. Blank-value pixels were written out if the test failed. This rather stringent test was necessary to prevent spurious fits to noisy data. All fits were independent in the sense that no "memory" of the RM of an adjacent pixel was used to assist in the determination. In all regions where a solution was made, the data fitted a λ^2 dependence to within the expected error. In Figure 2 we show eight typical fits, demonstrating the extremely good λ^2 dependence.

V. RESULTS

The results of these observations are best displayed graphically. Figure 3 shows the rotation measure maps, based on the least-squares fit to the position angle data. This image shows a number of outstanding new features. Most immediate are the large values in both the rotation measure and in its gradient over both lobes. For the eastern lobe, the RM varies from < -3000 rad m^{-2} to $> +4000$ rad m^{-2}, while for the western lobe, the range is from -2000 to $+1500$ rad m^{-2}. It is also striking that the RM increases from east to west in both lobes,

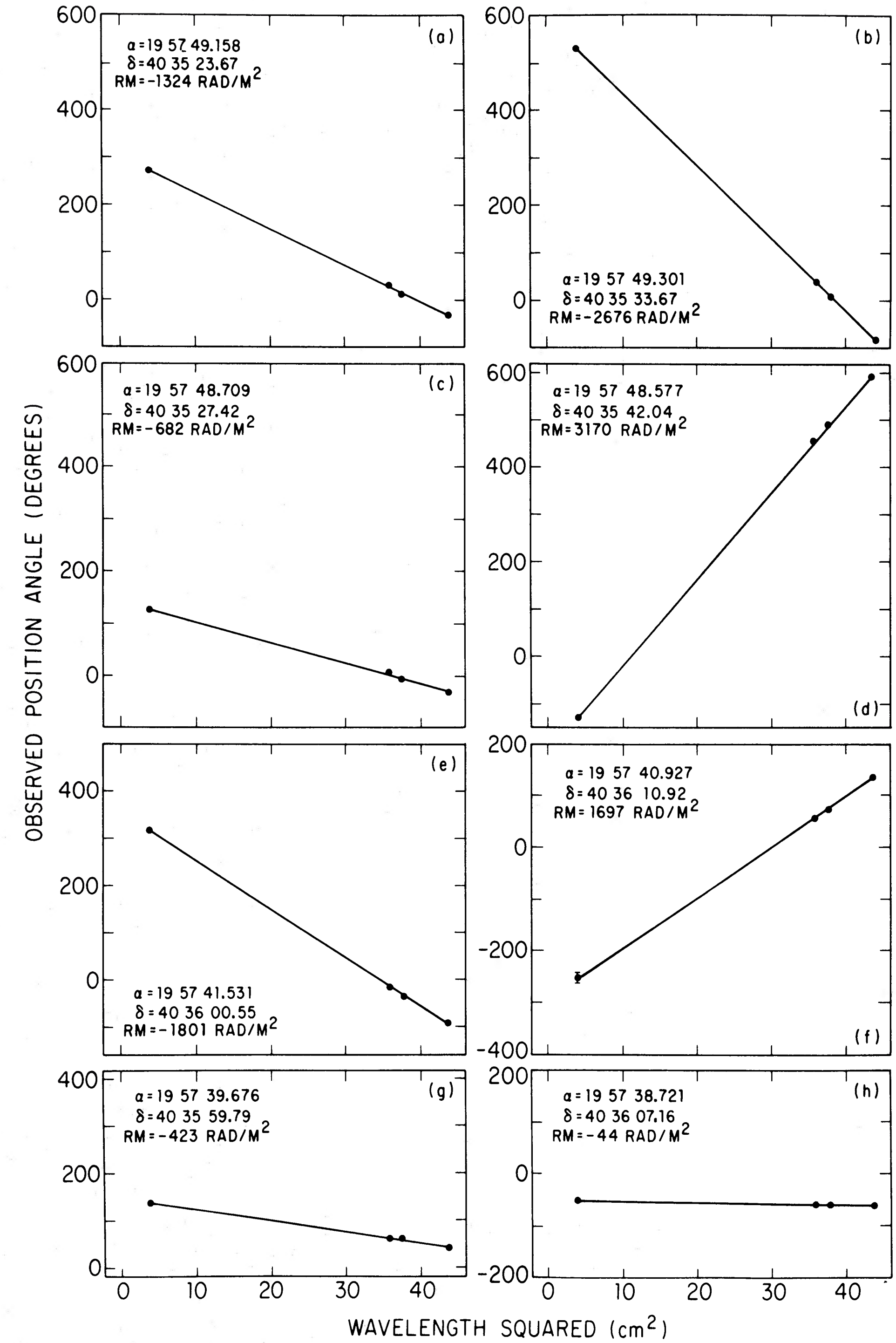

FIG. 2.—Examples of the fits of χ vs. λ^2 at eight locations in Cygnus A. Each point is plotted with its error bar—in most cases, the errors are smaller than the plotted dots. The coordinates and best fitting slope are printed inside each box.

so that the large-scale gradient lies roughly along the axis of the radio source. Unfortunately, the lower values of polarized brightness throughout most of the eastern lobe (only the hot spot and leading edge of this lobe have appreciable polarized brightness at 5 GHz) prevent calculation of the RM in a good part of this region, so detailed analysis of the large-scale variation, especially with respect to symmetry between the lobes, is not possible. Nevertheless, it is clear that there is a large-scale reversal of the sign of the RM over each lobe—this requires a reversal in the line-of-sight magnetic field, since density fluctuations alone cannot cause a sign reversal unless we are willing to postulate a flat, foreground contribution exceeding 3000 rad m^{-2}. As this postulate can be safely rejected, we must conclude that the magnetic field reverses direction on a $\sim 20''$–$40''$ scale. The large-scale ordering of the magnetic fields is probably an important clue to the origin of these fields; we,

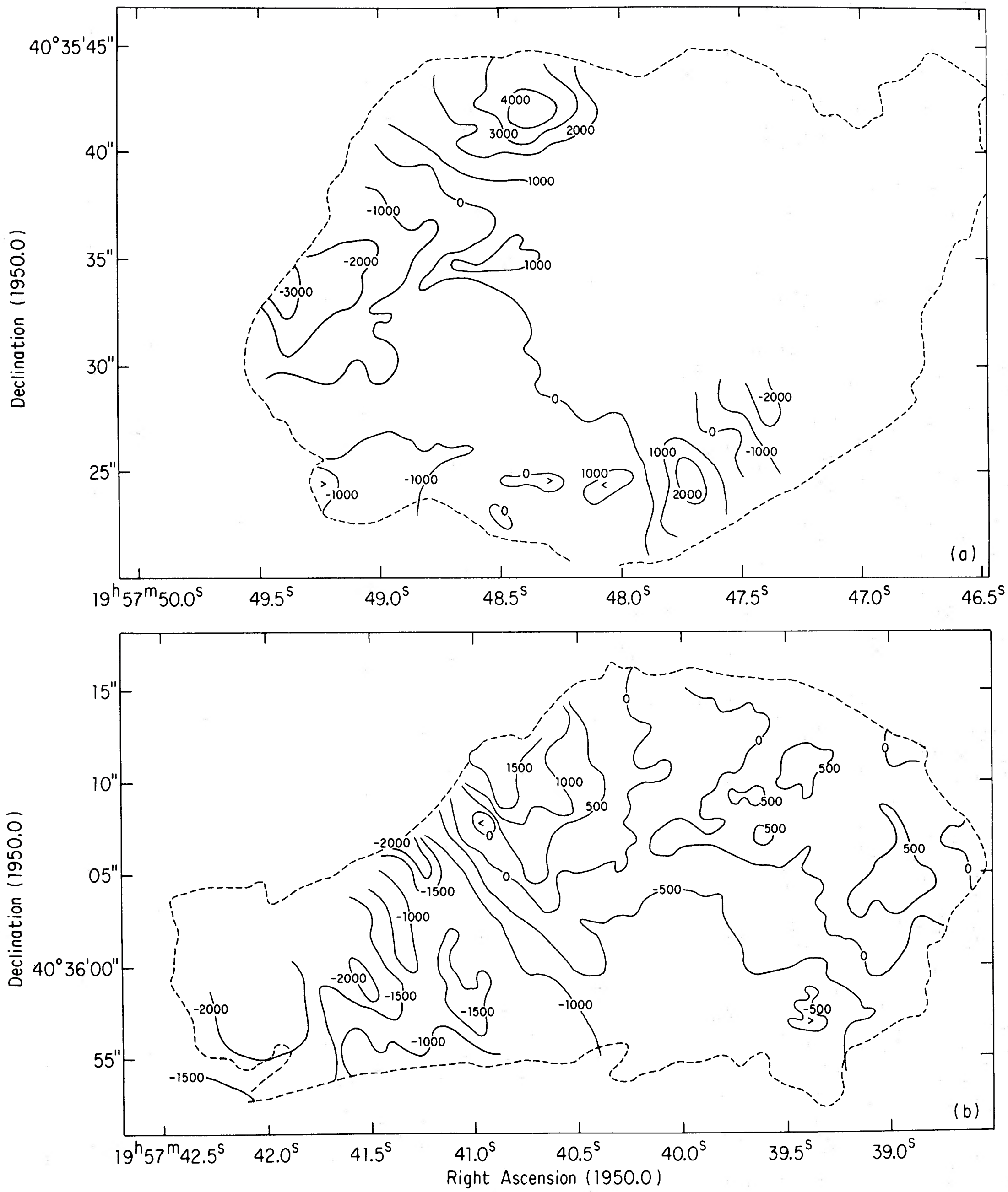

FIG. 3.—The distribution of rotation measure for Cygnus A, derived as explained in the text. The dashed line gives the boundaries of the radio lobes. Contour lines that end within the lobes indicate regions in which insufficient polarized brightness exists to determine the rotation measure. In particular, note that no fits were possible throughout nearly half the eastern lobe. The situation in the western lobe is much better.

unfortunately, have not yet been able to decipher it. It is also intriguing that a somewhat similar ordering of the RM occurs across the source M84 (Laing and Bridle, in preparation), although the scale here is much less than in Cygnus A.

On a smaller scale, very large gradients are present in many regions. The largest is in the eastern lobe, with a change of 7000 rad m^{-2} occurring over an angular scale of 10" along the northern edge of the lobe. As expected, beam depolarization at 5 GHz is seen in this region. The region of this extreme RM gradient is also prominent as a bright ridge on the edge of the intensity map. If these features are truly related, then we might be seeing evidence of mixing of the cluster gas into the edges of the radio lobe (as considered in § V*c*). Similar gradients, involving smaller changes over smaller angular distances, occur in both lobes, and gradients exceeding 300 rad m^{-2} arcsec^{-1} are common.

The explanation of the rotation measure anomaly is straightforward. At high frequencies ($\nu > 5$ GHz), where the early measurements are concentrated, the radio emission, because of spectral index effects, primarily originates in the regions around the hot spots. In these regions, the RM is indeed approximately -1000 rad m^{-2} for the eastern lobe, and ~ 0 rad m^{-2} for the western. The "tails," which have very different RMs, and steep spectral indices, contributed very little to these integrated measures. Thus, the lack of sufficient resolution and sensitivity led to an erroneous interpretation of the data.

A comparison of total intensity images with the RM maps reveals no noticeable correlation between the two quantities. Similarly, there is little correlation between polarized intensity and rotation measure, except in regions of high RM gradient, where beam depolarization occurs.

a) Evidence for an External Faraday Screen

As discussed in § IV, and shown in Figure 2, the fit of position angle, χ, to λ^2, is excellent. The fits displayed are typical for all pixels, with residuals generally within the expected noise in the position angles, and with no discernible deviations from λ^2 dependence. In many cases the plane of polarization at 5 GHz has been rotated by $\geq 600°$ from its intrinsic position angle. Recalling the general result (see Appendix A) that internal Faraday effects cannot cause a total rotation of observed position angle in excess of 90°, without very high depolarization, we are forced to the conclusion that the vast majority of the observed RM is due to an external Faraday screen and is not a result of gas internal to the radio source. Any contribution to the Faraday rotation by such gas must be a small perturbation on top of the huge external contribution, and is best investigated through measures of the depolarization.

b) Depolarization

As discussed in Δ IV, the depolarization ratio, D, could be accurately determined only when the input data had high signal-to-noise ratios, and in the absence of any strong changes in position angle. These requirements prevented any reliable measure of D in the eastern lobe. Fortunately, many regions of the western lobe did allow a meaningful evaluation of the ratio. We thus evaluated the depolarization ratio, $D = m_6/m_2$, only when the signal-to-noise ratio exceeded 30 (which should result in an error in D of less than ~ 0.05), and where gradients in RM or changes in intrinsic position angle would not cause beam depolarization. Subject to these restrictions, we found no evidence of depolarization. The regions in which this applies are located eastward of the "A" hot spot, where the RM is approximately 0 rad m^{-2}, and from this region toward the "B" hot spot. A straightforward average of the resulting depolarization ratio gave $D = 0.97 \pm 0.15$ rad m^{-2}. The high error is probably due to the noise in the degree of polarization maps being higher than a naive calculation (based on propagation of noise) gives. Such errors could be due to residual calibration errors (including effects of antenna pointing errors, known to be large during these observations at 15 GHz), deconvolution errors, or frequency-dependent effects within the source.

Even in the absence of signal-to-noise ratio and beam-depolarization effects, the interpretation of depolarization is model dependent. Consider a simple "slab" model, in which $B_{\|}$ and n_e are taken as constant along the line of sight. This configuration is the most "efficient" one in the sense that it produces the greatest Faraday depolarization for a given mean $B_{\|}$ and n_e. Other, and probably more realistic, models will generally require a larger mean n_e to produce the same depolarization. Thus, if we believe that a measured depolarization ratio represents the effects of internal Faraday depolarization, then we obtain a model-independent *lower limit* on n_e. Unfortunately, our observations of Cygnus A have provided only an *upper limit* on the possible internal depolarization. Since an upper limit on a lower limit is no limit at all, we can, therefore, obtain no *model-independent* limits on n_e.

By assuming particular models for the configuration of n_e and B, we can, of course, obtain model-dependent upper limit to n_e from our limits on D. The various models, however, can lead to drastically differing limits, as can be seen from the following three examples:

1. For a slab model with $B_{\|} = B_{\mathrm{eq}}$ and $L = 15$ kpc, we find $n_e < 2 \times 10^{-4}\ \mathrm{cm}^{-3}$.

2. For an *isotropic* random magnetic field varying on scale d with variance $\frac{2}{3}B_r^2$ superposed on a uniform B_z, Burn (1966) showed that the slab model dependency can be used, providing $B_r F_c/B_z \ll 1$, where F_c is the Faraday depth of a single cell. This condition certainly applies (for no appreciable polarized flux density could result at all if it did not), so it remains to determine B_z. Burn also showed that under the same conditions, the intrinsic degree of polarization is lowered by a ratio (uniform magnetic energy)/(total magnetic energy). Since the 15 GHz degree of polarization is about one-third the theoretical maximum (e.g., $\sim 25\%$), it follows that the inferred thermal gas density limit is of order $3^{1/2}$ greater than the naïve estimate given above, i.e., $\leq 4 \times 10^{-4}\ \mathrm{cm}^{-3}$.

3. For a strongly anisotropic random magnetic field, much larger values of n_e are possible. For example, Laing (1980) has shown that for a field configuration in which B_x and B_y are random, and $B_z \ll B_x \approx B_y$ (such as could conceivably occur upon compression of an initially isotropic random distribution along one axis), the intrinsic polarization, when viewed in the (x, y) plane, is precisely that expected for a uniform, completely ordered field. However, the depolarization will be reduced from the uniform case by a factor of order $N^{1/2}$, with N the number of field reversals along the line of sight. Thus, the appearance of a completely ordered field will result, in which a considerable amount of ionized gas can be "hidden," compared to the truly uniform situation. Similar considerations apply to sheared field configurations, where initially circular loops of magnetic field become stretched out by a velocity gradient. The result is again an appearance of ordered large-scale fields, with high degrees of polarization, but where the rate of depolarization is drastically reduced from the uniform field case. For both of these cases, the rate of depolarization, compared with the slab model, depends on the correlation spectra of the "random" fields. Regrettably, current theories are not yet developed to the point of providing useful information on the expected depolarization "efficiency" of the field configuration of sources like Cygnus A. It is not implausible, however, to imagine values of n_e one or two orders of magnitude larger than those found for the first two models.

Finally, it has been suggested that the lobes of radio sources like Cygnus A might be filled with an electron-positron plasma (e.g., Burns and Lovelace 1982; Morison, Roberts, and Sadun 1984; Williams 1986). In this case, no Faraday rotation or depolarization would occur. Note, however, that if in addition to the e^+e^- plasma, there are protons whose charge is balanced by electrons, then the Faraday rotation will depend on $n_{\mathrm{electron}} - n_{\mathrm{positron}} = n_{\mathrm{proton}}$. In this case, the presence of internal Faraday effects would still provide information on n_p and the mass density inside the lobes.

c) Projected Magnetic Field Structure

A final feature derivable from the polarization observations is the projected magnetic field structure of the source. This quantity comes from the zero-wavelength extrapolation of the fit used to derive the rotation measure, plus 90°. The results are shown in Figure 4. Of special interest is the clear tendency of the projected field to follow the boundaries of the source and

1987ApJ...316..611D

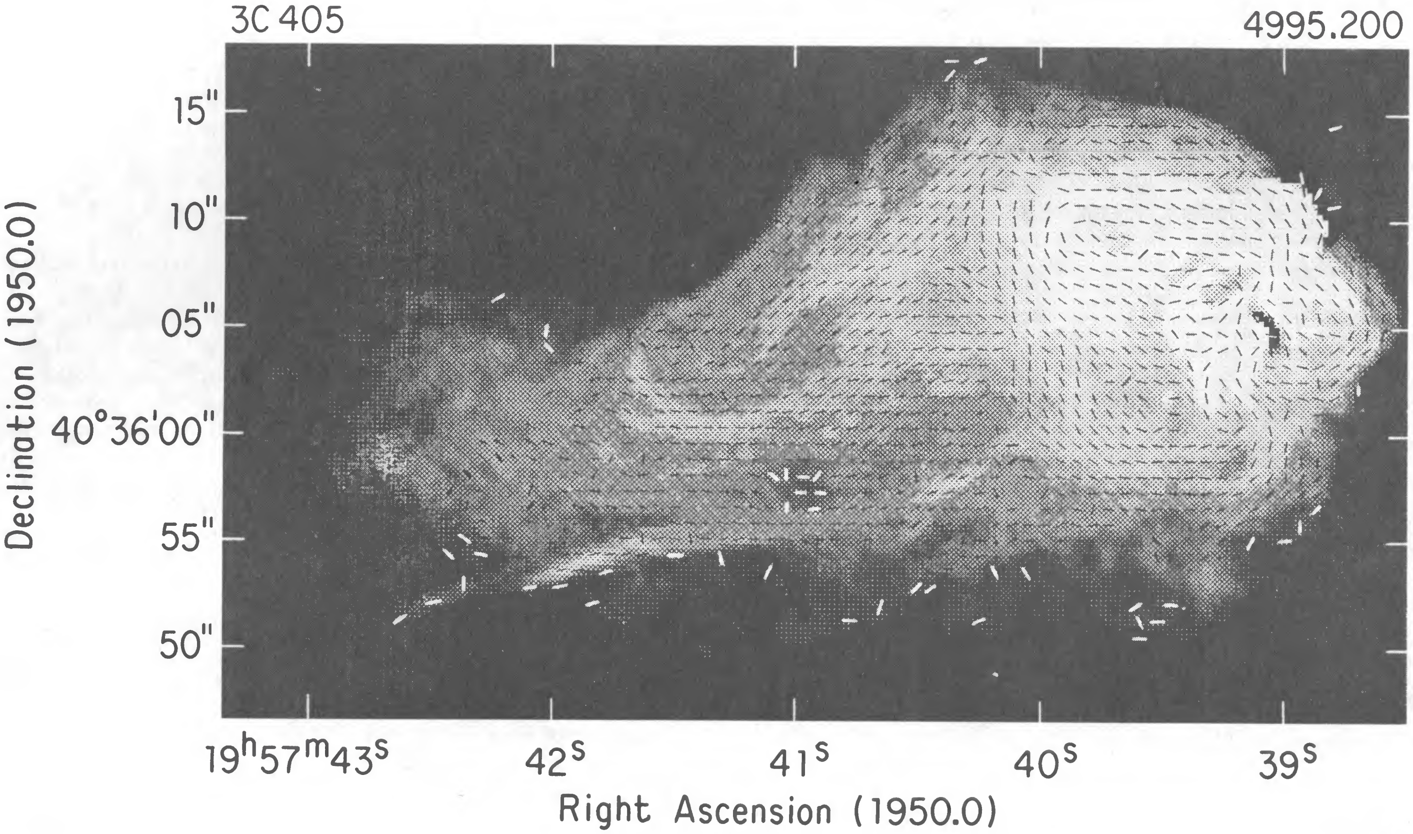

FIG. 4*a*

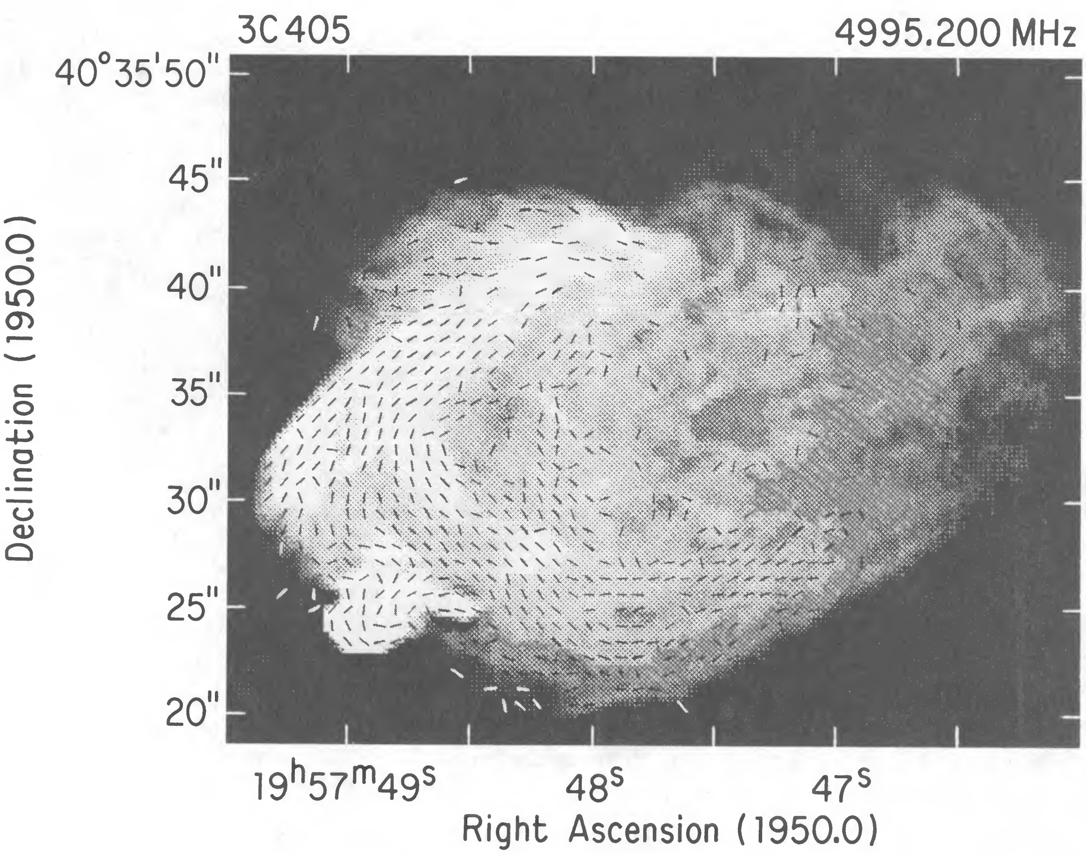

FIG. 4*b*

FIG. 4.—The distribution of intrinsic, projected magnetic field throughout the lobes in Cygnus A. The dashed lines are of unit length and lie parallel to the projected magnetic field. They are superposed onto a gray-scale image of the total intensity to show the excellent correlation between the direction of the field and the presence of bright loops of emission, and to the boundaries of the radio source.

the bright loops of emission in the western lobe. This is in excellent agreement with results on other extragalactic radio sources (e.g., 3C 382, Strom, Willis, and Wilson 1978; 3C 219, Perley *et al.* 1980; 3C 236, Strom and Willis 1980; 3C 326, Willis and Strom 1978; 3C 382, Burch 1979; 3C 111, 192, 219, 223, 315, 452, Hogböm 1979; NGC 6251, Perley, Bridle, and Willis 1984). Further, the implied magnetic field in the jet is longitudinal, in agreement with results from other high-luminosity sources (Bridle and Perley 1984; Bridle 1984; Bridle, Perley, and Henrikson 1986). These results strengthen our confidence that we have correctly removed the effects of the foreground screen.

The projected field behavior in the internal tail regions of the lobes is more ambiguous. At first glance, it appears the fields are generally parallel to the "filamentary" structures extending down the lobes (notably, the long thin filament in the western lobe tail, north of the jet). However, it is not clear if we have both filaments and fields independently extended along a single, preferred direction, and thus appear correlated, or if the fields are physically related to the filaments. In addition, while the direction of the magnetic field clearly follows some features of the brightness distribution (e.g., the prominent loop near $\alpha = 19^h57^m39^s.2$, $\delta = 40°36'00''$), there are also a few regions for which this behavior is less clear (e.g., the large loop centered near $\alpha = 19^h57^m39^s.7$, $\delta = 40°36'09''$). Note, however, that there is no apparent correlation between the projected field and the RM distribution.

VI. LOCATION AND NATURE OF THE FARADAY SCREEN

a) In Our Galaxy

The low Galactic latitude of Cygnus A ($b = 5.^\circ8$) has been used as the fundamental argument for a Galactic origin for the Faraday rotation. It has also been suggested by Alexander *et al.* that the large gradient in H I column density across Cygnus A found in the H I absorption study of Greisen might support the conclusion that the large gradients seen in RM could also be of galactic origin, although they make no attempt to justify the association.

The extraordinarily high RMs and RM gradients we find render this hypothesis less attractive for a number of reasons:

1. The magnitudes of the RM of extragalactic sources seen through the galaxy are generally found to be less than 300 rad m^{-2} down to $|b| \approx 3°$, much less than the RMs seen toward Cygnus A. More explicitly, there are 15 sources in the catalog of Simard-Normandin, Kronberg, and Button (1981) with $|b| < 15°$, and within 15° of Cygnus in galactic longitude. Of these, 13 have $|\mathrm{RM}| < 260$ rad m^{-2}. The other two are near $l = 91°$, $b = 0°$, and have $|\mathrm{RM}| < 360$ rad m^{-2}. In addition, we have determined the RM of our calibrator to be -139 ± 5 rad m^{-2}. This object is only $1.^\circ8$ away from Cygnus A and at a lower galactic latitude.

2. The small-scale fluctuations in RM that we see in Cygnus A are far larger than those seen in any other source, Galactic or extragalactic. Recent studies by Simonetti and Cordes (1986) on small-scale variations in RM seen in four extragalactic sources at low galactic latitude near longitude 90° show gradients in RM of less than ~ 100 rad m^{-2} on $0.'1$–$1'$ scales. Also, Higgs and Vallée (1986) report that the RM of the obscured extragalactic source 3C 428 ($l = 90.^\circ5$, $b = 1.^\circ3$) changes between lobes by only 80 rad m^{-2}, with a mean value of -320 rad m^{-2}.

3. For a class of extragalactic radio sources with unusually high RMs, in which Cygnus A is the most extreme member, Kronberg and Simard-Normandin (1976) have shown that the RMs are not correlated with galactic latitude. Thus, for most of the objects in this class at least, high RMs are *not* due to Faraday rotation in our Galaxy. They conclude that the origin of high RMs in extragalactic sources must be associated with the sources themselves.

4. The only Galactic objects known to give rise to such large values of RM as seen in Cygnus A are H II regions. Heiles, Chu, and Troland (1981, hereafter HCT) have determined the RMs of S117 and S119 to be -1100 and -2140 rad m^{-2}, respectively. There was little gradient in RM in either case (over angles of 9'' and 26''). They also found substantial emission measures for these regions (2600 and 1470 cm^{-6} pc, respectively). In comparison, only the faintest trace of red emission can be seen on the POSS near (but not coincident with) Cygnus A, far less than seen for either of these diffuse H II regions. We have recently made observations of the Hα emission in front of Cygnus A; our preliminary analysis indicates an EM < 300 rad m^{-2} (details will be published elsewhere). In addition, there is much more conspicuous red emission on the POSS at the position of our calibrator, even though we know it has a relatively small RM. Finally, the diffuse red emission near Cygnus A can be compared to that of the faint Hα emission region 2 of Sivan (1974), for which Simard-Normandin and Kronberg (1980) estimate an associated RM anomaly of ~ 200 rad m^{-2}.

It is instructive to estimate the physical parameters of a hypothetical galactic H II region that would fit all the data. The points discussed above require it to have a low emission measure, but a high RM. Since 2005+403 does not share the high RM, we estimate the angular radius of the region to be less than $\theta \approx 1.^\circ8$. This estimate, coupled with the 50 pc scale height, h_{OB}, above the Galactic plane for OB associations (Mihalas and Binney 1981), yields a linear diameter for the region, $L < 2h_{\mathrm{OB}} \csc(b_{\mathrm{II}}) \sin(\theta) \approx 30$ pc. We also require that the $\mathrm{RM} = 8.1 \times 10^5 n_e BL$ be >4000 rad m^{-2} and the emission measure, $\mathrm{EM} = n_e{}^2 L < 300$, a fairly generous upper limit. Assuming uniform magnetic fields and a uniform n_e along the line of sight will yield the least EM and maximum RM. The upper limit on n_e is $(\mathrm{EM}/L)^{1/2} \approx 3$ cm^{-3}, and the corresponding lower limit on B is $1.2 \times 10^{-6}(\mathrm{RM})(\mathrm{EM})^{-0.5} L^{-0.5} \approx 60$ μG. An H II region with this density and size would be classified as a "giant" in the scheme of Habing and Israel (1979) and is rather similar to the region S264, with EM = 250, studied by HCT, except for the magnetic field: this is more than an order of magnitude above that found for S264. The ratio of magnetic to thermal energy for the hypothetical H II region would be >10 as compared to values generally $\ll 1$ for the regions studied by HCT (see their eq. [1]). Also, since the actual faint filaments of red emission seen on the POSS near Cygnus A have widths very much less than $1.^\circ8$, this model of the hypothetical H II region probably underestimates the B field required by a large factor.

We conclude that if the RM arises in a foreground H II region in our Galaxy, then this region must be very unusual. The chances of finding such an oddity in front of the brightest extragalactic radio source seem remote.

b) In the Intracluster Medium

The idea that large-scale gas surrounding the radio source might be responsible for the rotation measure was dismissed by Mitton because it required clouds of ionized gas whose mass must exceed 10^{11} $M_{\odot}$, a mass considered unreasonable at the time. However, as noted in § II, X-ray observations have shown that Cygnus A is, indeed, at the center of a very large mass (10^{14} $M_{\odot}$) of such gas (Fabbiano *et al.* 1979; Arnaud *et al.* 1984). This gas provides a natural candidate for the magnetoactive region responsible for the Faraday screen. In addition to providing the necessary electrons, it is not unreasonable that the characteristic size scales of the intracluster medium (ICM) might be similar to those of the radio source, and it is certain that the ICM is strongly influenced by the gravitation of the parent galaxy of Cygnus A, which might account for some of the large-scale ordering of the RM (see § V).

Against this explanation stands the general belief that the gas in clusters contributes an RM of no more than $\sim 10^2$ rad m^{-2} (Sarazin 1986). Observationally, this estimate is based on three lines of evidence. First, from a study of the polarization of radio sources seen within or through 12 Abell clusters of richness 0 to 2, Lawler and Dennison (1982) determined that the component of RM due to the clusters has an rms value ≤ 50 rad m^{-2} (the highest RM in their sample was only 130 rad m^{-2}). It is not clear, however, that this result is applicable to the kind of "cooling flow" clusters in which Cygnus A resides. Second, Valée, MacLeod, and Broten (1986*a*) have reported an excess RM of ~ 120 rad m^{-2} for three background sources seen through A2319. Third, and perhaps somewhat more relevant to Cygnus A, the RMs seen across the low-luminosity radio galaxy Virgo A (= M87) are also believed to be much less than those we find for Cygnus A, even though Virgo A is immersed in a dense halo of X-ray emitting gas. From observations at 2.7 and 8 GHz, DeYoung, Hogg, and Wilkes (1979) reported RMs over Virgo A of ≤ 116 rad m^{-2}, while from a comparison of optical polarization in the jet with the 5 GHz data of Turland (1975), Schmidt, Peterson, and Beaver (1978) inferred RMs of ≥ 360 rad m^{-2}. Dennison (1980) reanalyzed these observations and those of Forster *et al.* (1978) at 23 GHz to conclude that the RM arising in the X-ray emitting gas has a value ~ 460 rad m^{-2}. We feel, however, that the polarization data on Virgo A must be approached with caution in light of the enormous RMs across Cygnus A. In order to avoid the same problems that earlier led to estimates of ~ 100 rad m^{-2} for the western lobe of Cygnus A (more than an order of magnitude too low!), both an angular resolution sufficient to resolve the basic structures of the source and a frequency coverage that includes very small ranges in $\delta\lambda^2$ are vital. Unfortunately, currently published observations of Virgo A do not meet these stringent requirements. It should also be noted that the X-ray emitting gas in the Cygnus A cluster is ~ 5 times as dense as that in the Virgo A halo at 100 kpc, the radius pertinent to our observations. All in all, then, while the idea of RMs > 1000 rad m^{-2} through clusters of galaxies is startling, it cannot be ruled out for those with the densest ICMs.

Not only do present observations not rule out large RMs in cooling flow clusters, but there may be another example in the source 4C 26.42, studied by van Breugel, Heckman, and Miley (1984). This low-luminosity, edge-darkened radio galaxy is inside the cooling flow cluster Abell 1795 which is at about the same distance from us as Cygnus A. Their 5 GHz map shows almost no linear polarization at a resolution of 1"3, while at 0"3 resolution small patches of 10%–30% polarization appear. This behavior is strongly reminiscent of that seen in our maps and may well have the same explanation—that is, large RM gradients have generated beam depolarization. Van Breugel *et al.* were unable to determine the RM distribution over 4C 26.42, but, based on the low polarization and the detection of optical emission from $\sim 10^4$ K gas, they suggested the presence of a lumpy external Faraday screen. (They considered models which identify this screen with a region localized around the lobes; we consider this hypothesis in § VI*c* below.)

We have considered a number of models that relate the cluster field strengths to the observed RM distribution and to the cluster density profile derived from the X-ray data. A lower limit to the mean line-of-sight field can be found by integrating the density profile from the radio lobes to the edge of the cluster assuming a constant B field aligned with the line of sight. This yields $B > 2$ μG. More plausibly, the field may vary with the density, although our understanding of cluster fields is yet too underdeveloped to give much guidance on how. For concreteness, we have considered two cases, $B \propto n^{2/3}$ (flux conservation) or $B \propto n^{1/2}$ (magnetic energy scales with the thermal energy). In either case, the estimate of the mean line of sight field increases to ~ 3 μG. We also considered quasi-random walks through "cells" of field within the cluster gas, with cellular fields of constant strength and random direction. This yields values for the most probable fields of 5–12 μG for cell sizes ranging from 50 to 10 kpc, respectively. Note, however, that neither model can reproduce the observed large-scale structure of the RM distribution. To accomplish this, we considered loops of field centered on the galaxy. This yields field values of ~ 7 μG within the loops. Note that for all these derived fields, the total magnetic energy is only of order 1% of the thermal energy, so there appears to be little chance of the fields influencing cluster dynamics. Details of these models are presented in Appendix B.

These cluster magnetic fields are somewhat higher than those previously suggested in the literature. From considerations of limits to the cluster contribution to the RMs of extragalactic sources, Lawler and Dennison (1982) obtained an upper limit to intracluster fields of $B < 0.35$ μG. From models of diffuse radio halos, cluster fields of ~ 1 μG are estimated (Sarazin 1986 and references therein). Vallée, MacLeod, and Broten (1986*b*) suggest a mean field of ~ 0.2 μG for A2319, or, under the more likely scenario of looped fields within cells of 20 kpc scale, a strength of 2 μG. Lastly, an upper limit to any possible homogeneous field pervading all of intergalactic space was found by Ruzmaikin and Sokoloff (1977) to be ~ 0.001 μG.

That the fields we estimate are higher may not be surprising in view of the unusual nature of the Cygnus A cluster. First, it seems likely that the magnetic field and density of a cluster are related and, consequently, that the cluster RM may depend strongly on the density. For example, if $B \propto n^{2/3}$ then RM $\propto nB = n^{5/3}$. Comparing Cygnus A and Virgo A, we would then expect the RM for Cygnus A to exceed that for Virgo A by $\sim 5^{5/3} \approx 15$, which is consistent with the reported values (see above). Second, the presence of Cygnus A in the cluster might also account for the relatively high magnetic fields. However, if the observed radio lobes are expanding hyper-Alfvénically and supersonically into the ICM, as their appearance suggests (Paper II), then they cannot directly have affected the cluster gas as a whole. We can, however, *speculate* on two possible mechanisms by which Cygnus A could have magnetized its cluster. First, previous outbursts of the radio source may have created lobes that have expanded by now into invisibility but left behind magnetic "fossils" into which the cluster gas may have mixed. Second, cD galaxies are often held to have grown by cannibalism, and, if this is true for the Cygnus A parent, then the magnetic fields of the victim galaxies, like ghosts, may have accumulated in the inner part of the ICM.

c) *In a Sheath Surrounding the Lobes*

The last hypothesis for the location of the Faraday screen that we shall consider is that it lies in a dense layer of gas immediately exterior to the radio lobes, which we denote the "sheath." This hypothesis has two attractive features. First, in the standard picture of radio source dynamics, the lobes are expanding supersonically with respect to the external gas. Just outside the leading edge of the lobe, a bow shock is expected to form inside of which the thermal gas density and magnetic fields will be enhanced. The post–bow-shock region that forms around the lobe is then a good candidate for the Faraday screen. Second, the immediate contact of the sheath and the lobe provides a natural explanation for the roughly lobe-scale features found in the RM distribution. Evidence for enhanced densities surrounding radio lobes has been provided by detection of optical emission from the radio lobes of several objects (van Breugel, Heckman, and Miley 1984 and references therein). They find that this dense, $\sim 10^4$ K gas is preferentially located on the peripheries of the lobes and, further, that it may be associated with regions of low radio polarization. They propose that these regions are depolarized by the Faraday rotation either of the observed cool gas or of a hot, thermally unstable gas from which this cool gas condensed.

A less attractive aspect of this hypothesis is that it requires magnetic fields of $\sim 100\ \mu$G in the sheath. We can estimate the field in two ways. First, since the bow shock is believed to be both strong and adiabatic, a density jump of 4 is expected across the shock. At the radius of the hot spots, the unperturbed density of the ICM is $\sim 5 \times 10^{-3}$ cm^{-3}; thus, the density in the sheath should be $\sim 2 \times 10^{-2}$ cm^{-3}. From the hydrodynamic simulations of supersonic jets made by Norman *et al.* (1982) and by Williams and Gull (1984), it appears that the thickness $l_{\rm sheath}$ of the shocked layer is ~ 1 kpc. To obtain the RM of -2000 rad m^{-2} observed at the eastern hot spot (knot "D") then requires a minimum magnetic field of 120 μG. The second method of estimating B follows from consideration of the total amount of ICM that must have been displaced by a lobe. Using the observed density profile and a simple cylindrical geometry with diameter 20 kpc and extending radially from 10 kpc to 65 kpc yields a rough estimate of $10^{10}\ M_\odot$ for the mass displaced. If we divide this mass by the surface area of the lobe, an estimate of the column density through the sheath is found, which is also a rough estimate for $n_e l_{\rm sheath}$. Numerically, this yields $n_e l_{\rm sheath} \approx 0.1$ cm^{-3} kpc, and to obtain an RM ~ 2000 rad m^{-2} then requires $B \geq 40\ \mu$G.

Simple compression of the magnetic field of the ICM in the bow shock would be expected to increase the magnetic field strength by a factor ≤ 4, depending on the geometry. To produce the high fields required for the sheath would, therefore, require B fields in the ICM considerably higher than those required under the hypothesis of § VI*b* above. This means that if the only source of magnetic field is the intrinsic field of the ICM, then the cluster as a whole should produce larger RMs than the shocked ICM in the sheath. For the sheath to be the dominant source of the RM, another source of field is necessary. The obvious candidate is the $\sim 100\ \mu$G magnetic field inside the lobe (assuming equipartition; Paper I). The edges of the lobes present an appearance in several places that is suggestive of mixing by instabilities (e.g., the edge north of the eastern hotspot; see Fig. 1 of Paper I). If the thermal electrons of the ICM can diffuse onto the intense fields of the lobes in these regions, then it might be possible to create a suitable Faraday screen. Of course, this mixed layer must not penetrate very far into the synchrotron-emitting region, lest it cease acting as a Faraday screen (Cioffi and Jones 1980).

VII. SUMMARY

The principal results concerning the polarization properties of Cygnus A, based on multiconfiguration VLA images at 4.525, 4.885, 4.995, and 14.7 GHz with a resolution of 0″.35 are as follows:

1. At all points across Cygnus A, the rotation of the position angle of the plane of polarization is proportional to λ^2 to within the measurement errors. The total rotation, at our lowest frequency, exceeds 600° in many areas, forcing the conclusion that the effect is due to an external screen of magnetized, ionized gas.
2. The RMs seen over the source are larger than seen in any other extragalactic source by a large margin. They range from -4000 rad m^{-2} to $+3000$ rad m^{-2}. Further, the small-scale gradients in RM are larger than ever seen in any other radio source. Both these large gradients and the absence of any optical emission from ionized gas rule out an origin of the RM within our galaxy.
3. The two lobes have similar large-scale RM distributions. The gradient in each lies along the radio axis. Each exhibits a large range in RM, but the eastern lobe has larger values and gradients. Reversals of the fields over scales of typically 20–40 kpc are required for each lobe.
4. No evidence for intrinsic depolarization between 5 and 15 GHz is found. Some apparent depolarization occurs in regions of high gradient in RM due to beamwidth effects. The deduced internal thermal gas density limits are model-dependent.
5. The most likely location for the screen is near the radio source, either in the dense, X-ray emitting cluster gas, or in a denser sheath around the lobes. In either case, the magnetic fields are higher than expected: $\sim 5\ \mu$G for the ICM or $\sim 10^2$ μG for the sheath. The origin of these fields is obscure.

Our discovery of very large RMs over Cygnus A creates a puzzle. Why is Cygnus A so different than other extragalactic radio sources in regards to its RM? We point out three factors. First, Cygnus A is embedded in a dense, "cooling flow" cluster. If this is the important factor, other dense clusters should show similar RMs. The available evidence is mixed, but does not rule out this hypothesis. Second, Cygnus A is an extraordinarily luminous radio galaxy. This factor, by itself, is unlikely to be important, as RMs for other luminous sources, not embedded in dense regions, show no RM irregularities. Again, however, there are few data. Third, the combination of the above factors may be important. However, note that if Cygnus A has somehow magnetized all or part of the cluster, it must do so in spite of the likelihood that the lobes are expanding supersonically and super-Alvénically.

To better understand the phenomenon, more mapping of the rotation measures of extragalactic radio sources is needed. In particular, detailed observations of other radio sources embedded in dense X-ray emitting clusters are required. This is lengthy and painstaking work, but, we feel, it may well yield new insight into the interaction of radio sources with their environments.

One of us (R. A. P.) is grateful for the pleasant environment and hospitality of the staff of the Dominion Radio Astrophysical Observatory, where much of this paper was written.

APPENDIX A

DEPOLARIZATION OF RADIATION BY FARADAY DISPERSION

In this section, we briefly review some aspects of the theory of propagation of electromagnetic radiation through a magneto-ionic medium in terms of the Stokes parameters I, Q, and U. A more complete treatment of the fundamental equations will be found, for example, in Pacholczyk (1970). The results shown are also found in Cioffi and Jones (1980).

For quasi-longitudinal propagation in the high-frequency limit, the equations of transfer for Stokes parameter I, and complex polarized flux density P, defined in terms of the Stokes parameters as $P = Q + iU$, are

$$\frac{dI}{ds} = -\kappa I + \epsilon \tag{A1}$$

$$\frac{dP}{ds} = 2i\beta P - \kappa P + f(\gamma)\epsilon e^{2i\chi_B} . \tag{A2}$$

In these expressions, we have assumed that the thermal gas does not radiate and that the relativistic electron energy distribution is power law, $N(E) = N_0 E^{\gamma}$, and isotropic in pitch angle. The direction of the projected magnetic field at depth s referred to the observer's coordinate frame is denoted χ_B, and β is the rate of change of the position angle of polarized flux density with path length; in c.g.s. units for an electron-proton gas, $\beta = 2.62 \times 10^{-17} n_e B_{\parallel} \lambda^2$, where $B_{\parallel}$ is the line-of-sight component of the magnetic field at depth s. The mean emission coefficient is denoted ϵ, and $f(\gamma) = (3\gamma + 3)/(3\gamma + 7)$. At the frequencies of interest, thermal absorption can be ignored, so these equations give the well-known solutions

$$I = \int_0^L \epsilon ds \tag{A3}$$

and

$$P = P_0 e^{F(L)} + e^{F(L)} \int_0^L f(\gamma)\epsilon e^{-F(s')} ds' . \tag{A4}$$

P_0 is the polarized intensity incident on the region of interest, and $F(x)$ is given by $F(x) = \int_0^x 2i\beta ds$. In terms of the Faraday depth, $\phi(x)$, $F(x) = 2i\lambda^2\phi(x)$. We consider two special cases of particular interest.

1. *The Foreground Screen.*—In this case, the radiation from a background source passes through a screen of magnetized thermal gas. Then, $f(\gamma)\epsilon = 0$, so the polarized flux density becomes $P = P_0 e^{2i \int \beta ds}$. From this it is seen that the polarized intensity, $|P|$, is unchanged upon emergence, but that the position angle, $\chi = \frac{1}{2}$ arctan (U/Q), is rotated by $\delta\chi = \int_0^L \beta ds$. Converting to units convenient in astrophysics, we find

$$\delta\chi = 0.81\lambda^2 \int_0^L n_e \boldsymbol{B} \cdot \boldsymbol{ds} , \tag{A5}$$

where $\delta\chi$ is in radians, γ is the wavelength in meters, n_e is the thermal gas density in cm^{-3}, $\boldsymbol{B}$ is the magnetic field in μG, and s is the path length in parsecs. $\delta\chi(\lambda)$ is the total rotation of the plane of polarization for radiation traversing the length of the screen. It is proportional to λ^2, with the constant of proportionality known as the rotation measure, RM.

Although these equations show that the polarization intensity is not changed, this situation pertains only when the resolution is sufficient to resolve the transverse variations in the screen. In the more usual case, where there is structure at or smaller than the instrumental resolution, a drop in polarized flux density will be noted. This situation (commonly known as *beam depolarization*) must be carefully distinguished from the true depolarization due to thermal gas in the emitting region (see next section). The only effective test is to vary the resolution and see if the depolarization changes. Beam depolarization is especially troublesome since its effects are strongest at the longer wavelengths where the diffraction-limited resolution of the instrument cannot resolve out the responsible screen.

2. *Intermixed Polarized Emission and Thermal Absorption.*—This is a much more complicated case, and we consider in detail only the *slab model.* Here, all variables are uniform through the source, which we take to have depth L. We can in this case, without loss of generality, rotate the reference frame to make $\chi_B = 0$ and find

$$P = \frac{f(\gamma)\epsilon}{2i\beta} (1 - e^{-2i\beta L}) . \tag{A6}$$

The degree of polarization, $m = |P|/I$, is given by

$$m = f(\gamma) \left| \frac{\sin(\beta L)}{\beta L} \right| . \tag{A7}$$

The polarized flux density is cyclical with depth, as emission from different depths suffers differing degrees of rotation upon propagation to the front. These differing rotations interfere, causing the net polarization to depend sinusoidally with depth. However, the total intensity is not affected by the rotation, so the degree of polarized flux density drops. The observed position angle becomes

$$\chi = \frac{1}{2} \arctan \left| \frac{\sin \beta L}{\cos \beta L} \right| . \tag{A8}$$

The position angle of polarized flux density again follows a λ^2 law, but with two important differences from the simple screen. The rate of rotation is now half that of the simple screen, that is, $-\beta L/2$, and the position angle is constrained to lie between 0 and $-\pi/2$. Cioffi and Jones (1980) have studied other simple models and reached the same conclusion. Thus, a plot of the position angle versus βL will show a slope of $-\frac{1}{2}$, until $\beta L = \pi$, at which the position angle changes discontinuously from $-\pi/2$ to 0. The resulting plot is sawtooth.

Burn (1966) has considered important generalizations of the internal depolarization. If the field within the source contains a random component, denoted B_r, with Gaussian distribution, on scales of d, superposed on an overall uniform field, B_z, then the intrinsic (zero-wavelength) polarization is lowered by the ratio of the energy in the uniform field to that in the total magnetic field. In the slab model, inclusion of this type of random field results in a degree of polarization given by

$$m(\lambda^2) = m_i \frac{1 - e^{-S}}{S} , \tag{A9}$$

where

$$S = N F_r^{\,2} - 2iF_z . \tag{A10}$$

Here, $N = L/d$, the number of cells through the line of sight; F_r is the Faraday rotation due to a random cell ($F_r = \beta_r d$); and F_z is the Faraday rotation through the source due to the mean field ($F_z = \beta_z L$). The behavior of S depends on the ratio of the real and imaginary parts. The imaginary part dominates when the rotation within one cell due to the random field component is much less than that occurring over the same length due to the mean field. Note that the relative importance of real and imaginary parts is a function of wavelength, since the random component enters raised to the second power. When the imaginary part dominates, the results of the "smooth" slab model are recovered, with the important difference that the intrinsic degree of polarization is reduced by the factor noted above. When the real part dominates, the degree of polarization drops dramatically. This dramatic drop is the best indicator of internal Faraday depolarization. Burn gives examples of the behavior of the polarized intensity and position angle for various combinations of the real and imaginary parts of the parameter S.

Burn also considers models with spherical geometry. However, for our purposes, it is adequate to consider only the simpler slab model. This is because our observations resolve out the transverse variations completely, so the line-of-sight field components are the important quantity. The most important conclusion to be had from his models is that the internal depolarization case cannot give rise to more than $\pi/2$ rotation in the plane of polarized flux density.[6] Thus, if any radio source shows more than this rotation in its plane of polarization, the inevitable conclusion is that the origin must be external. The question of a limit on the internal component can only be simply answered by measuring the depolarization ratio. However, because the depolarization is dependent upon the direction of the magnetic field, derivations of values, or limits, to the internal thermal gas density require an assumption of the magnetic field geometry. This point has been made especially clear by the work of Laing (1980) as outlined in example 3 of § V*a*. Laing (1984) has reviewed the difficulties of interpreting polarization data.

APPENDIX B

ESTIMATES OF INTRACLUSTER MAGNETIC FIELDS

We present here details of the models employed to estimate the magnetic field strengths within the Cygnus A cluster. These estimates assume the observed Faraday rotation of polarized radiation from the Cygnus A radio sources is caused by the ambient ionized cluster gas. Note that the magnitudes of the intracluster fields derived below presume the gas is external to the radio source, so that no part of the observed rotation is due to gas within the radio emitting regions, where equipartition fields in excess of 100 μG are found (Paper I).

The radial electron density profile, $n_e(r)$, for the Cygnus A cluster, as taken from the X-ray observations (Arnaud *et al.* 1985), has the form (scaled to $H = 75$ km s^{-1} Mpc^{-1}):

$$n_e(r) = Ar^{-1.2} , \tag{B1}$$

where $A = 1.06$, r is in kpc, and n_e is in cm^{-3}. This equation is valid from approximately 50 kpc radius out to about 1 Mpc. Using $n(r)$ in equation (A5) above, with the RM values presented in this paper, we can determine the magnitude of the intracluster magnetic fields. However, due to the vector nature of B in equation (A5), any such estimates are highly sensitive to assumed field geometry. Below, we derive cluster field strengths for a variety of geometries. All calculations assume $H = 75$ km s^{-1} Mpc^{-1}: conversion to other values of H is easily accomplished by multiplying the desired values by $(H/75)^{1/2}$.

[6] This is not a general result. Pathological geometric arrangements can give $\delta\chi > 90°$. For instance, if the perpendicular component of the magnetic field were to rotate in perfect synchronism with the propagating radiation, which is rotating due to thermal Faraday effects (i.e., a spiraling field whose pitch varies with the internal thermal gas density), then no Faraday depolarization would occur at all! However, this case is obviously sharply frequency dependent, gives zero intrinsic polarization, and an indeterminate rotation measure.

The simplest class of models employs unidirectional magnetic field geometries. Integrating $B(x)n_e(x)$, where x is a position on the line of sight through the cluster, and $B(x)$ is the line-of-sight component of the magnetic field, then yields the (density-weighted) mean line-of-sight component of the field in the cluster. Choosing the RM of the southern hot spot, for example (RM = −2000 rad m^{-2}), equation (A5) becomes (assuming the radio source is in the plane of the sky):

$$-2000 = 0.81A \int_0^{10^3} B(x)(x^2 + 3600)^{-0.6} dx \,. \tag{B2}$$

An absolute lower limit to B is obtained if we let $B(x) = B_0$, a constant throughout the cluster. This yields $B_0 = 1.9\ \mu$G. We can also consider fields which scale with the electron density, $B(x) = Kn_e{}^m$. If we assume flux conservation, by analogy with the ISM, we have $m = \frac{2}{3}$, and the derived cluster magnetic field strength (at a cluster radius of 60 kpc, the outer edge of the radio source) is 3.5 μG. Alternatively, if we let the magnetic energy density scale with the thermal energy density, we have $m = \frac{1}{2}$, and we find $B = 3.1\ \mu$G. Again the above models depend upon fields which remain ordered throughout the length of the cluster, without reversals. The fields inferred should be considered only as lower limits to the cluster fields, since any anti-aligned segment of field negates a portion of the properly aligned field path length.

Our second class of models addresses the possibility of field reversals along the line of sight through the cluster to the source. The mechanism employed is a quasi-random walk through a number of field reversals, with the number of steps determined by the size of the region, or "cell" within which we consider the field to be ordered. If we assume a "correct" direction for the innermost cell (i.e., + or − field as determined by the sign of the RM observed), then we can random walk our way out of the cluster through the remaining $N - 1$ cells, with cell size = (cluster radius)/$N \approx 1/N$ Mpc, electron density given by equation (B1), and cellular magnetic field of constant magnitude and random direction. This yields for the most probable line-of-sight cluster magnetic field strengths 10.6, 6.7, 5.5 and 4.9 μG for cell sizes of 10, 20, 33, and 50 kpc, respectively. Notice the field strength becomes less sensitive to cell size for larger cells. This is due to the decline in electron density with radius, which makes the RM contribution of the innermost cell more dominant as the cell size increases.

Previous estimates of the coherence length for fields within rich clusters range from 1 to 20 kpc (see § V*b* above). This would imply line-of-sight fields greater than 6 μG for the Cygnus A cluster, given the above models. Recall, however, that Cygnus A lies is a fairly poor cluster (Spinrad and Stauffer 1982) and also exhibits a large X-ray cooling flow. The combined effects of these properties on cluster field cell sizes is unknown. The RM maps shown here show regions of coherent sign that range in size from 5 to 30 kpc, which could be an indication of typical cluster field cell sizes. However, the overall RM profile (as discussed in § IV) does not appear completely random, as would be expected for this model, but exhibits a fairly smooth large-scale structure across each lobe. A model based on this observation is considered next.

The most prominent coherent feature on the RM maps is the negative-to-positive variation in RM on going from east to west across each lobe. A possible field geometry which would produce such a profile is two concentric "rings" of field, centered on the galaxy, with opposite field directions (see Fig. 1 in Sofue *et al.* 1985, for an example of the RM profile expected in such a field geometry). The thickness of each ring is assumed to correspond to the length scale of the RM sign reversals (∼20 kpc). Again, using the observed cluster electron density profile and the observed RM values, we find the ring field geometry requires fields of ∼7 μG. Field configurations of this type have been observed on smaller scales within the disks of spiral galaxies and are thought to arise from field shear and amplification due to differential rotation of gas within the disk. It seems unlikely that such a model should be applied to the essentially spherical distribution of gas which causes the X-ray emission. Another field geometry, leading to the same estimate of magnetic field strength, but with entirely different consequences, are loops of field, centered on each lobe, with ∼20 kpc scale size. Here, the problem is in understanding how the necessary large-scale currents can arise within the lobe and how the subsequently generated field can become infused with cluster gas.

REFERENCES

Alexander, P., Brown, M. T., and Scott, P. F. 1984, *M.N.R.A.S.*, **209**, 851.
Arnaud, K. A., Fabian, A. C., Eales, S. A., Jones, C., and Forman, W. 1984, *M.N.R.A.S.*, **211**, 981.
Baade, W., and Minkowski, R. 1954, *Ap. J.*, **119**, 206.
Baars, J. M. W., Genzel, R., Pauliny-Toth, I. I. K., and Witzel, A. 1977, *Astr. Ap.*, **61**, 99.
Bridle, A. H. 1984, *A.J.*, **89**, 979.
Bridle, A. H., and Perley, R. A. 1984, *Ann. Rev. Astr. Ap.*, **22**, 319.
Bridle, A. H., Perley, R. A., and Henriksen, R. N. 1986, *A.J.*, **92**, 534.
Burch, S. F. 1979, *M.N.R.A.S.*, **186**, 519.
Burn, B. F. 1966, *M.N.R.A.S.*, **133**, 67.
Burns, M. L., and Lovelace, R. V. E. 1982, *Ap. J.*, **262**, 87.
Cioffi, D. F., and Jones, T. W. 1980, *A.J.*, **85**, 368.
Clark, B. G. 1980, *Astr. Ap.*, **89**, 377.
Cornwell, T. J., and Evans, K. F. 1985, *Astr. Ap.*, **143**, 77.
Dennison, B. 1980, *Ap. J.*, **236**, 761.
DeYoung, D. S., Hogg, D. E., and Wilkes, C. T. 1979, *Ap. J.*, **228**, 43.
Dreher, J. W. 1979, *Ap. J.*, **230**, 687.
Dreher, J. W., Perley, R. A., and Cowan, J. J. 1984, in *Physics of Energy Transport in Extragalactic Radio Sources, Proc. NRAO Workshop 9*, ed. A. H. Bridle and J. A. Eilek (Green Bank, W. Va.: NRAO), p. 57 (Paper 11).
Fabbiano, G., Doxsey, R. E., Johnston, M., Schwartz, D. A., and Schwartz, J. 1979, *Ap. J. (Letters)*, **230**, L67.
Forster, J. R., Dreher, J. W., Wright, M. C. H., and Welch, W. J. 1978, *Ap. J. (Letters)*, **221**, L3.
Greison, E. W. 1973, *Ap. J.*, **184**, 379.
Habing, H. J., and Israel, F. P. 1979, *Ann. Rev. Astr. Ap.*, **17**, 345.
Hargrave, P. J., and Ryle, M. 1974, *M.N.R.A.S.*, **166**, 305.
Heiles, C., Chu, Y. H., and Troland, T. 1981, *Ap. J. (Letters)*, **247**, L77 (HCT).
Higgs, L. A., and Vallée, J. P. 1986, *J.R.A.S. Canada*, **80**, 180.
Hogböm, J. A. 1974, *Astr. Ap. Suppl.*, **15**, 417.
——— 1979, *Astr. Ap. Suppl.*, **36**, 173.
Kileen, N. E. B., Bicknell, G. V., and Ekers, R. D. 1986, *Ap. J.*, **302**, 306.
Kronberg, P., and Simard-Normandin, M. 1976, *Nature*, **263**, 653.
Kronberg, P., Van den Bergh, S., and Button, S. 1977, *A.J.*, **82**, 315.
Laing, R. 1980, *M.N.R.A.S.*, **193**, 439.
——— 1984, in *Physics of Energy Transport in Extragalactic Radio Sources, Proc. NRAO Workshop 9*, ed. A. H. Bridle and J. A. Eilek (Green Bank, W. Va.: NRAO), p. 90.
Lawler, J. M., and Dennison, B. 1982, *Ap. J.*, **252**, 81.
Mihalas, D., and Binney, J. 1981, *Galactic Astronomy* (San Francisco: Freeman), p. 252.
Mitton, S. 1971, *M.N.R.A.S.*, **153**, 133.
Mitton, S., and Ryle, M. 1969, *M.N.R.A.S.*, **146**, 221.
Morrison, P. M., Roberts, D., and Sadun, A. 1984, *Ap. J.*, **280**, 483.
Norman, M. L., Smarr, L., Winkler, K.-H. A., and Smith, M. D. 1982, *Astr. Ap.*, **113**, 285.
Osterbrock, D. E., and Miller, J. S. 1975, *Ap. J.*, **197**, 535.
Pacholczyk, A. G. 1970, *Radio Astrophysics* (San Francisco: Freeman).
Perley, R. A., Bridle, A. H., and Willis, A. G. 1984, *Ap. J. Suppl.*, **54**, 291.

Perley, R. A., Bridle, A. H., Willis, A. G., and Fomalont, E. B. 1980, *A.J.*, **85**, 49.
Perley, R. A., Dreher, J. D., and Cowan, J. J. 1984, *Ap. J.* (*Letters*), **285**, L35 (Paper I).
Ruzmaikin, A. A., and Sokoloff, D. D. 1977, *Astr. Ap.*, **58**, 247.
Sarazin, C. L. 1986, *Rev. Mod. Phys.*, **58**, 1.
Schmidt, G. D., Peterson, B. M., and Beaver, E. A. 1978, *Ap. J.* (*Letters*), **220**, L31.
Simard-Normandin, M., and Kronberg, P. P. 1980, *Ap. J.*, **242**, 74.
Simard-Normandin, M., Kronberg, P. P., and Button, S. 1981, *Ap. J. Suppl.*, **45**, 97.
Simkin, S. M. 1977, *Ap. J.*, **217**, 45.
Simmonds, J. F. L., and Stewart, B. G. 1985, *Astr. Ap.*, **142**, 100.
Simonetti, J. H., and Cordes, J. M. 1986, preprint.
Sivan, J. P. 1974, *Astr. Ap. Suppl.*, **16**, 163.
Slysh, V. I. 1966, *Soviet Astr.—A.J.*, **9**, 533.
Sofue, Y., Klein, U., Beck, R., and Wielebinski, R. 1985, *Astr. Ap.*, **144**, 257.
Spinrad, H., and Stauffer, J. R. 1982, *M.N.R.A.S.*, **200**, 153.
Strom, R. G. and Willis, A. G. 1980, *Astr. Ap.*, **85**, 36.
Strom, R. G., Willis, A. G., and Wilson, A. S. 1978, *Astr. Ap.*, **68**, 367.
Thompson, A. R., Clark, B. G., Wade, C. M., and Napier, P. J. 1980, *Ap. J. Suppl.*, **44**, 151.
Turland, B. D. 1975, *M.N.R.A.S.*, **170**, 281.
Vallée, J. P., MacLeod, J. M., and Broten, N. W. 1986*a*, *Astr. Ap.*, **156**, 386.
———. 1986*b*, preprint.
van Breugel, W., Heckman, T. and Miley, G. 1984, *Ap. J.*, **276**, 79.
van den Bergh, S. 1976, *Ap. J.* (*Letters*), **210**, L63.
Wardle, J. F. C., and Kronberg, P. P. 1974, *Ap. J.*, **194**, 249.
Williams, A. G. 1986, Ph.D. thesis, University of Cambridge.
Williams, A. G., and Gull, S. F. 1984, *Nature*, **310**, 33.
Willis, A. G., and Strom, R. G. 1978, *Astr. Ap.*, **62**, 375.

C. L. CARILLI and J. W. DREHER: Department of Physics, Massachusetts Institute of Technology, Cambridge, MA 02139

R. A. PERLEY: National Radio Astronomy Observatory, P.O. Box O, Socorro, NM 87801